Protein-template gold nanoclusters induce differentiation and modify the functional properties of primary astrocytes

Roberta Fabbri[1], Karima Jeneh Perry[2]*, Emanuela Saracino[1]*, Chiara Lazzarini[1,3], Anna Mariano[4], Diletta Spennato[1,3], Maria Grazia Mola[5], Maria Grazia Raucci[4], Alessandro Kovtun[1], Marianna Barbalinardo[6], Giorgia Conte[1], Denis Gentili[6], Marco Caprini[7,8], Vincenzo Palermo[1], Roberto Zamboni[1], Luigi Ambrosio[4], Wolfgang Losert[9], Andrea Candini[1]±, Grazia Paola Nicchia[3], Raj K. Gupta[10], Valentina Benfenati[1]±, Shashi P. Karna[2]±.*

[1] Institute for Organic Synthesis and Photoreactivity (ISOF), National Research Council of Italy (CNR), Bologna, Italy.

[2] DEVCOM Army Research Laboratory, ATTN: FCDD-RLA-A, Aberdeen Proving Ground, College Park, Maryland, USA.

[3] Department of Biosciences, Biotechnologies and Environment, University of Bari Aldo Moro, Bari, Italy.

[4] Institute for Polymers, Composites, and Biomaterials (IPCB), National Research Council of Italy (CNR), Mostra d' Oltremare, Napoli, Italy.

[5] Department of Medicine and Surgery, Libera Università Mediterranea "Giuseppe Degennaro", Casamassima, Italy

[6] Institute for the Study of Nanostructured Materials (ISMN), National Research Council of Italy (CNR), Bologna, Italy.

[7] Department of Pharmacy and Biotechnology, (FaBit), University of Bologna, Bologna, Italy.

[8] Istituto delle Scienze Neurologiche di Bologna, IRCCS, Bologna, Italy.

[9] Department of Physics, University of Maryland, College Park, Maryland, USA.

[10] DoD Blast Injury Research Coordination Office, Medical Research and Development Command, Fort Detrick, Maryland, USA.

[±]Corresponding authors Valentina Benfenati, Shashi P. Karna, Andrea Candini

valentina.benfenati@isof.cnr.it; shashi.p.karna.civ@army.mil; andrea.candini@isof.cnr.it

Supporting Information

Supporting Information is available from the Wiley Online Library or from the author.

Supporting Information

Protein-template gold nanoclusters induce differentiation and modify the functional properties of primary astrocytes

Roberta Fabbri[1], Karima Jeneh Perry[2]*, Emanuela Saracino[1]*, Chiara Lazzarini[1,3], Anna Mariano[4], Diletta Spennato[1,3], Maria Grazia Mola[5], Maria Grazia Raucci[4], Alessandro Kovtun[1], Marianna Barbalinardo[6], Giorgia Conte[1], Denis Gentili[6], Marco Caprini[7,8], Vincenzo Palermo[1], Roberto Zamboni[1], Luigi Ambrosio[4], Wolfgang Losert[9], Andrea Candini[1]±, Grazia Paola Nicchia[3], Raj K. Gupta[10], Valentina Benfenati[1]±, Shashi P. Karna[2]±.*

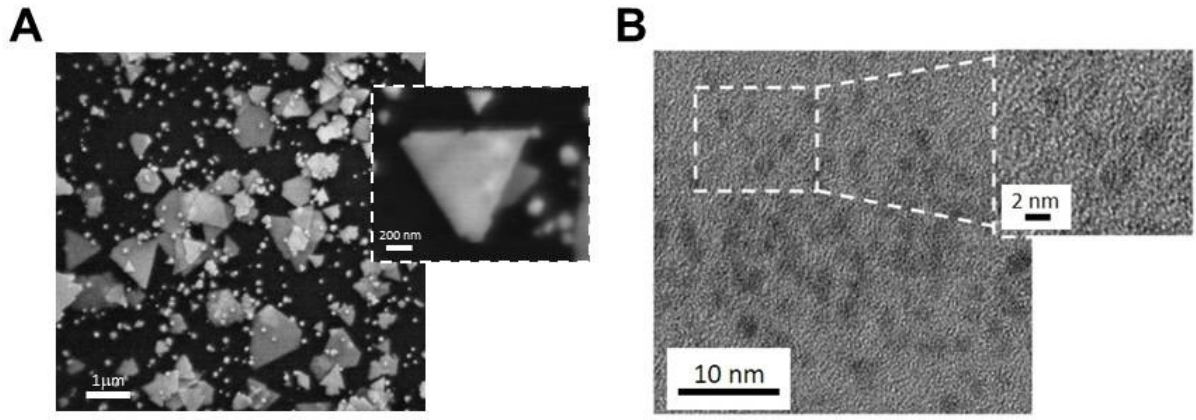

Figure Supplementary S1. Morphological properties of fAuNCs-BSA. A) Scanning Electron Microscopy (SEM) image of dried fAuNCs-BSA casted over a glass coverslip from cell media. Scale bar is 1 µm. Inset: higher magnification image, scale bar is 200 nm. B) Transmission Electron Microscopy image (TEM) investigation of the smallest particles of fAuNCs-BSA. Scale bar is 10 nm. Inset: higher magnification, scale bar is 2 nm.

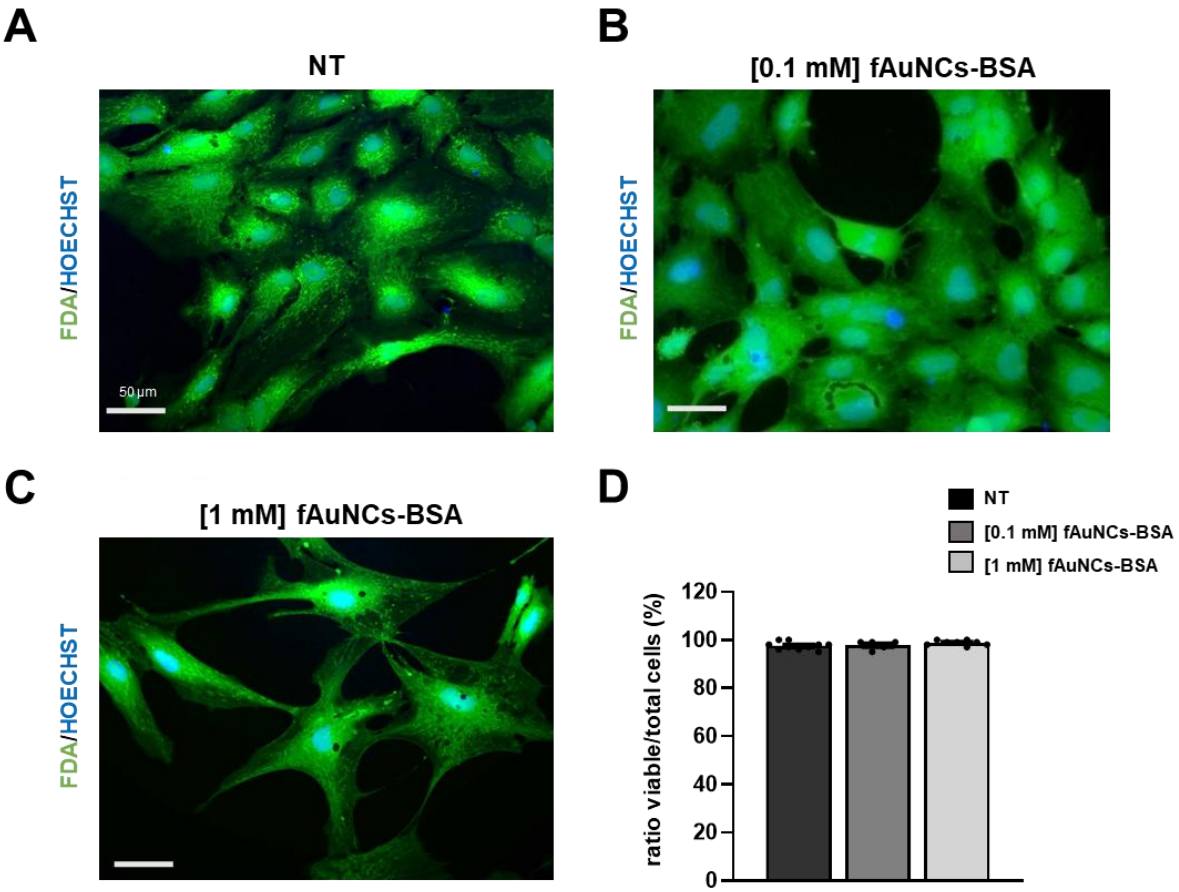

Figure Supplementary S2. Impact of fAuNCs-BSA on astrocyte viability and morphology. A, B, C) Low magnification (20X) confocal images of FDA/Hoechst stained astrocytes: NT (A), fAuNCs-BSA [0.1 mM] (B) and fAuNCs-BSA [1 mM] (C) treated cells captured at 3 DIV. Scale bar is 50 µm. D) Bar-dot plot reporting the ratio between the averaged fluorescence of viable cells and of the total number of cells per image (FDA^+-$Hoechst^+$/Total number of Hoechst+ cells) calculated on NT and fAuNCs-BSA [0.1 mM] and fAuNCs-BSA [1 mM] treated samples after 3 DIV. n=10 for NT, n=5 for fAuNCs-BSA [0.1 mM] and n=8 for fAuNCs-BSA [1 mM] (n= number of images analyzed). Data are reported as mean ± SE. Statistical significance was calculated via one-way ANOVA with Bonferroni post-test. *: $p< 0.05$, **: $p< 0.01$, ***: $p< 0.001$. No statistical difference was observed between NT and fAuNCs-BSA [0.1 mM] ($p=0.75$), between NT and fAuNCs-BSA [1 mM] ($p=0.08$) and between fAuNCs-BSA [0.1 mM] and fAuNCs-BSA [1 mM] ($p=0.24$).

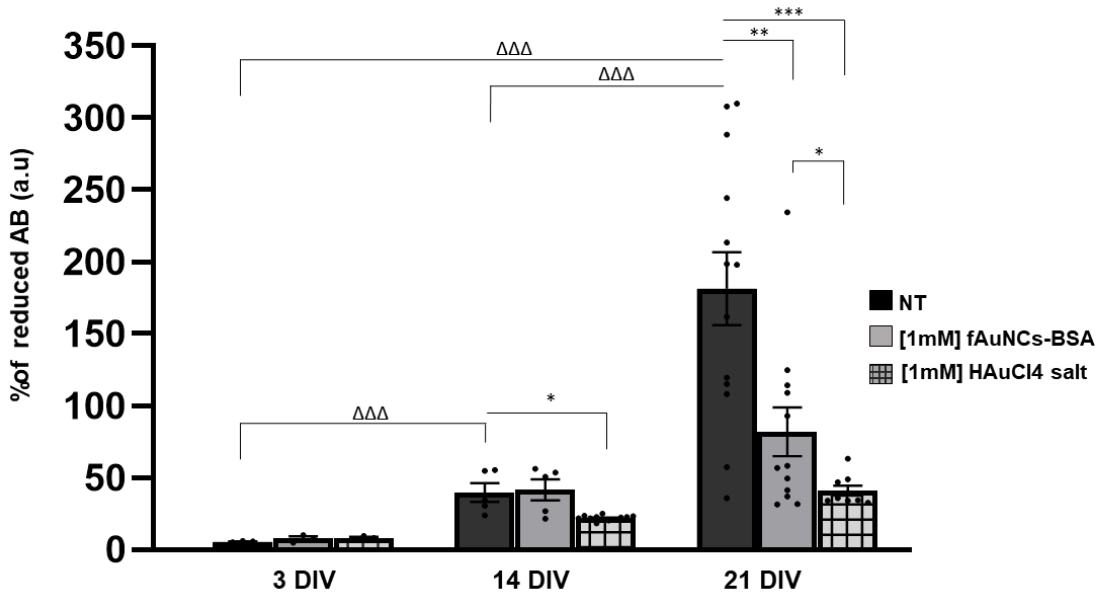

Figure Supplementary S3. Effect of fAuNCs-BSA on astrocyte metabolic activity. Bar-dot graph of percentage of reduced Alamar Blue, cell metabolism assay performed on NT, fAuNCs-BSA [1 mM] and HAuCl4 [1mM] treated astrocytes at 3DIV, 14DIV and 21 DIV. For 3 DIV, n=3 for NT, n=3 for fAuNCs-BSA [1 mM] and n= 3 for HAuCl4 [1mM]; for 14 DIV, n=5 for NT, n=5 for fAuNCs-BSA [1 mM] and n=12 for HAuCl4 [1mM]; for 21 DIV, n=13 for NT, n=12 for fAuNCs-BSA [1 mM] and n=9 for HAuCl4 [1mM] (n=number of measurements). Data are reported as mean ± SE. Statistical significance was calculated via one-way ANOVA with Bonferroni post-test. *: $p< 0.05$, **: $p< 0.01$, ***: $p< 0.001$. Statistical difference was observed in the % of reduced AB between NT and fAuNCs-BSA [1 mM] at 21 DIV ($p=0.0039$). No statistical difference was observed in the % of reduced AB between NT and fAuNCs-BSA [1 mM] at 3 DIV (0.24) and at 14 DIV (0.84). Statistical difference was observed in the % of reduced AB between NT and HAuCl4 [1mM] at 3 DIV ($p=0.05$), at 14 DIV ($p=5.83\ 10^{-4}$), at 21 DIV ($p=1.93\ 10^{-4}$). Statistical difference was observed in the % of reduced AB between fAuNCs-BSA [1 mM] and HAuCl4 [1mM] at 14 DIV ($p=14.26\ 10^{-4}$). No statistical difference was observed in the % of reduced AB between fAuNCs-BSA [1 mM] and HAuCl4 [1mM] at 3 DIV ($p=0.85$) and at 21 DIV ($p=0.06$).

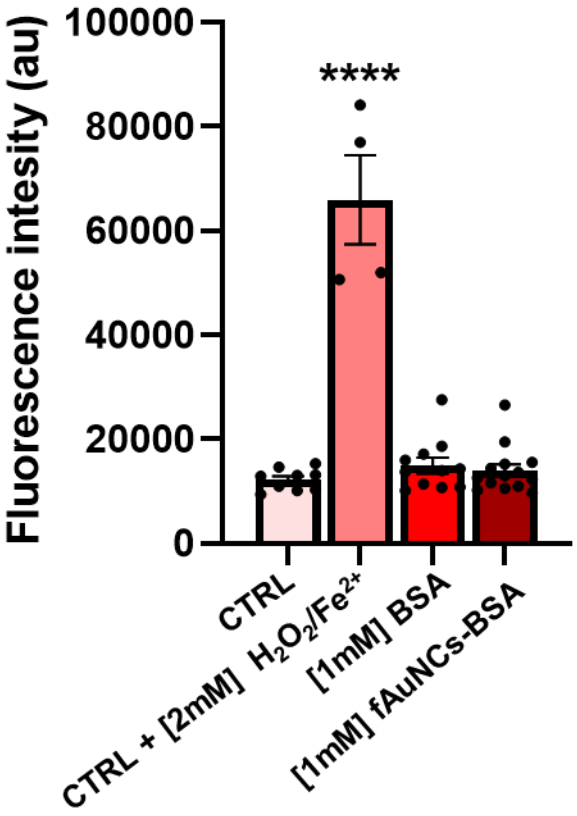

Figure Supplementary S4. fAuNCs-BSA is not inducing Reactive Oxygen Species (ROS). Averaged DCFH-DA fluorescence intensity, which correlates with the intracellular concentration of ROS.[1,2] Data are reported as mean ± SE (n = 3, n=number of experiments for each condition). Statistical significance was calculated via one-way ANOVA test with post hoc Dunnett's test. ****$p < 0.0001$.

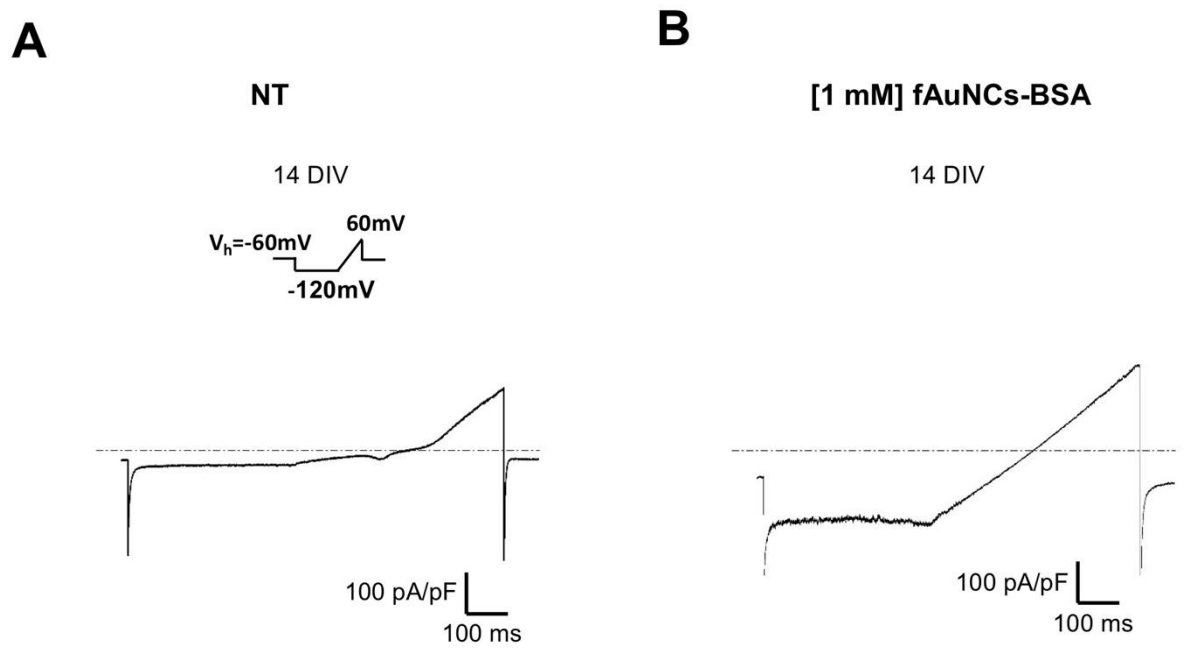

Figure Supplementary S5. Effect of fAuNCs-BSA on electrophysiological properties of astrocytes. Typical current traces recorded stimulating astrocytes with a voltage ramp protocol (inset to panel A) from -120 to +60 mV (500 ms) with Vh=-60 mV, in NT (A) and fAuNCs-BSA [1 mM] treated (B) astrocytes in standard condition (black line, CTRL) in presence of potassium in the intracellular and extracellular solution, at 14 DIV from the treatment with fAuNCs-BSA [1mM].

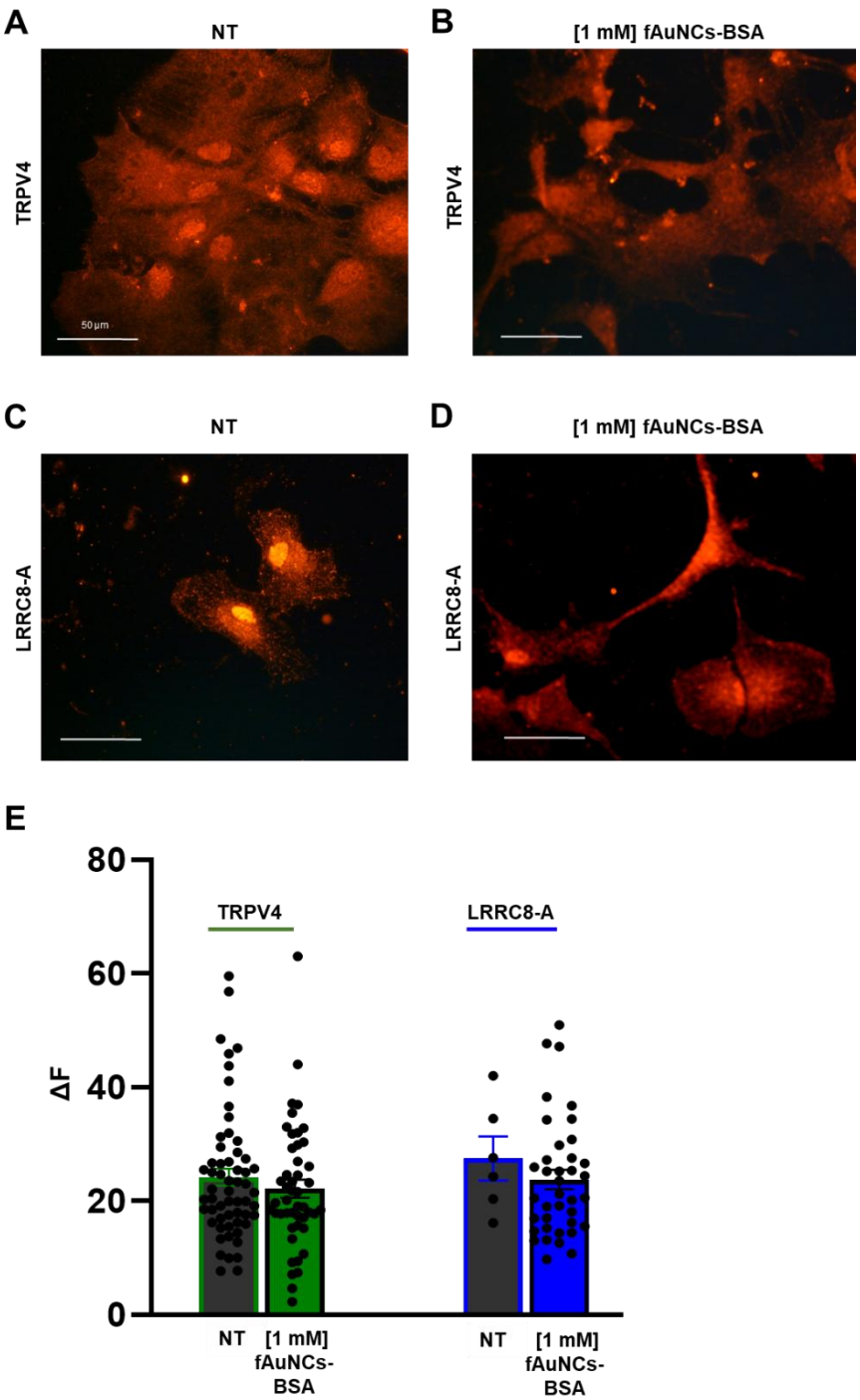

Figure Supplementary S6. Effect of fAuNCs-BSA on TRPV4 and LRRC8-A in astrocytes. Confocal microscopy images of primary cortical astrocytes stained with TRPV4 (A, B) and with LRRC8-A (C, D) antibodies in NT (A, C) and fAuNCs-BSA [1mM] treated (B, D) conditions. Scale bar is 50 µm. E) Bar-dot graph representing the quantification of averaged fluorescence variation measured in TRPV4 and LRRC8-A stained- astrocytes, in NT and fAuNCs-BSA [1mM] treated conditions. For TRPV4, n=58 for NT and n=47 for fAuNCs-BSA [1mM]; for LRRC8-A, n=6 for NT and n=38 for fAuNCs-BSA [1mM] (n=number of images analyzed). Data are reported as mean ± SE. Statistical significance was calculated via one-way ANOVA with Bonferroni post-test. *: $p< 0.05$, **: $p< 0.01$, ***: $p< 0.001$. No statistical difference was observed between NT and fAuNCs-BSA [1mM] for TRPV4 ($p=0.35$) and for LRRC8-A ($p=0.4$) -stained astrocytes.

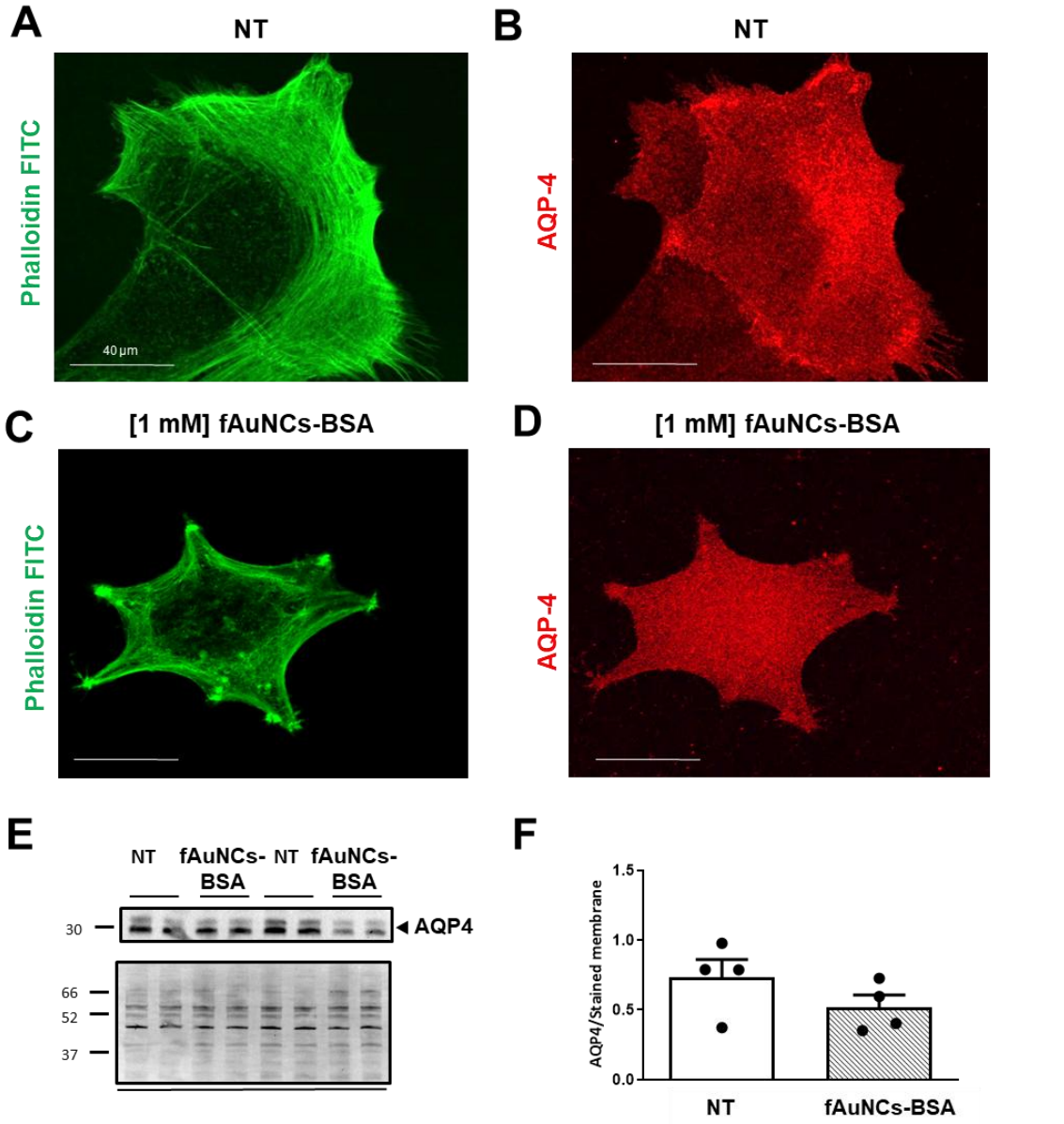

Figure Supplementary S7. Effect of fAuNCs-BSA on AQP4 expression in astrocytes. Confocal images of primary cortical astrocytes stained with FITC Phalloidin (green staining)/AQP4 (red staining) in NT (A, B) and fAuNCs-BSA [1mM] treated cells (C, D). The images show the response of astrocytes' morphology and cytoskeleton and the expression of the water channel AQP4 in NT (A, B) and fAuNCs-BSA [1mM] (C, D) treated cells. Scale bar is 40 µm. E, F) Representative western blot analysis of AQP4 expression in primary astroglial cultures in NT and fAuNCs-BSA [1mM] treated cells after 24hrs. The immunoblotting (E) and quantification of the expression level of AQP4 (F) notes that the expression level of AQP4 decrease, not significantly, between NT and fAuNCs-BSA treated astrocytes (n=4, n=number of experiments for each condition). Data are reported as mean ± SE. Statistical significance was calculated via one-way ANOVA with Bonferroni post-test. *: $p< 0.05$, **: $p< 0.01$, ***: $p< 0.001$.

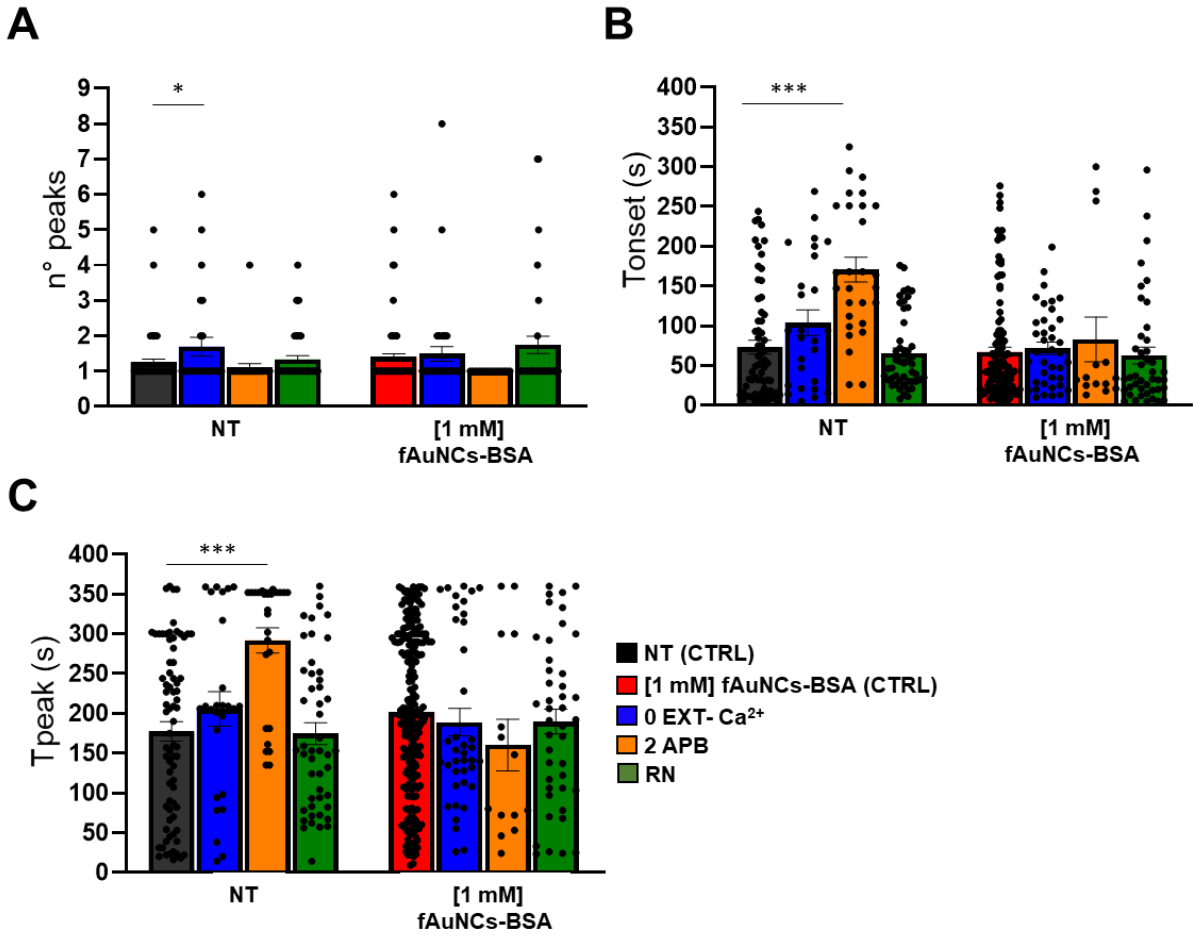

Figure Supplementary S8. Statistical analysis of calcium imaging experiments performed on NT cells and fAuNCs-BSA [1mM] treated cells, in standard extracellular solution (CTRL, black bar for NT and red bar for fAuNCs-BSA [1mM]), and under pharmacological treatment by removing calcium from the extracellular solution (0 EXT Ca^{2+}, blue bars) and upon the exposition to 2-Aminoethoxydiphenyl borate [100 µM] (2APB, inhibitor of IP_3, orange bars) and to RN-1734 [10 µM] (RN, inhibitor of TRPV4, green bars). A-C) Bar-dot graphs representative of the experiments conducted on astrocytes, showing A) averaged number of peaks, B) averaged onset time (s), C) averaged time to peak (s). For CTRL condition, n=75, N=9 for NT and n=230, N=9 for fAuNCs-BSA [1mM]. For 0 EXT Ca^{2+} condition, n=26, N=3 for NT and n=39, N=3 for fAuNCs-BSA [1mM]. For 2APB condition, n=17, N=3 for NT and n=14, N=3 for fAuNCs-BSA [1mM]. For RN condition, n=48, N=3 for NT and n=43, N=3 for fAuNCs-BSA [1mM] (n=number of cells, N=number of independent experimental trials). Data are reported as mean ± SE. Statistical significance was calculated via one-way ANOVA with Bonferroni post-test. *: p< 0.05, **: p< 0.01, ***: p< 0.001-
Statistical difference was observed in n° peaks between NT CTRL and NT 0 EXT-Ca^{2+} (p=0.045). No statistical difference was observed in n° peaks between NT CTRL and NT + 2APB (p=0.67), and between NT CTRL and NT + RN (p=0.5). No statistical difference was observed in n° peaks between fAuNCs-BSA [1mM] CTRL and fAuNCs-BSA [1mM] 0 EXT-Ca^{2+} (p=0.67), between fAuNCs-BSA [1mM] CTRL and fAuNCs-BSA [1mM] + 2APB (p=0.09), and between fAuNCs-BSA [1mM] CTRL and fAuNCs-BSA [1mM] + RN (p=0.09). No statistical difference was observed in n° peaks between NT CTRL and fAuNCs-BSA [1mM] CTRL (p=0.23). Statistical difference was observed in Tonset (s) between NT CTRL and NT+2APB (p=4.87 10^{-6}). No statistical difference was observed in Tonset (s) between NT CTRL and NT 0 EXT-Ca^{2+} (p=0.07), and between NT CTRL and NT + RN (p=0.5). No statistical difference was observed in Tonset (s) between fAuNCs-BSA [1mM] CTRL and fAuNCs-BSA [1mM] 0 EXT-Ca^{2+} (p=0.7), between fAuNCs-BSA [1mM] CTRL and fAuNCs-BSA [1mM] + 2APB (p=0.42), and between fAuNCs-BSA [1mM] CTRL and fAuNCs-BSA [1mM] + RN (p=0.7). No statistical difference was observed in Tonset (s) between NT CTRL and fAuNCs-BSA [1mM] CTRL (p=0.57). Statistical difference was observed in Tpeak (s) between NT CTRL and NT + 2APB (p=0.0002). No statistical difference was observed in Tpeak (s) between NT CTRL and NT 0 EXT-Ca^{2+} (p=0.25), and between NT CTRL and NT + RN (p=0.9). No statistical difference was observed in Tpeak (s) between fAuNCs-BSA [1mM] CTRL and fAuNCs-BSA [1mM] 0 EXT-Ca^{2+} (p=0.49), between fAuNCs-BSA [1mM] CTRL and fAuNCs-BSA

[1mM] +2APB (p=0.15), and between NT CTRL and NT + RN (p=0.5). No statistical difference was observed in Tpeak (s) between NT CTRL and fAuNCs-BSA [1mM] CTRL (p=0.08).

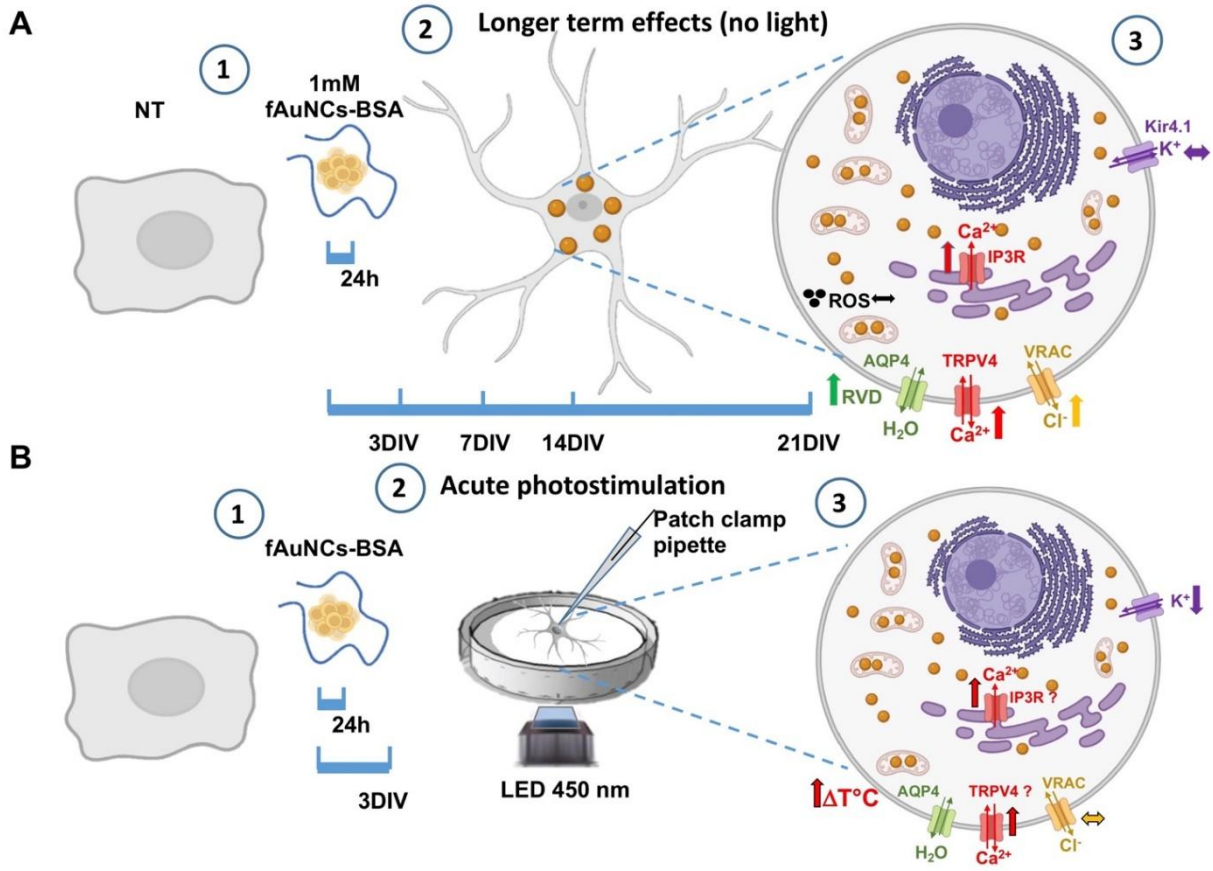

Figure Supplementary S9. Scheme of effects of [1mM] fAuNCs-BSA in astrocytes at different time points and of possible mechanism beyond. A) **1**-Scheme representing the protocol for treatment of astrocytes (NT) with [1mM] fAuNCs-BSA. **2-** Blue bar at the bottom represents different time points of morphological molecular and functional analyses performed to analyze effects of [1mM] fAuNCs-BSA with no light exposure over longer term. The scheme highlights that the treatment with fAuNCs-BSA leads to morphological differentiation of astrocytes. **3-** The treatment with fAuNCs-BSA does not induce ROS production (horizontal black arrow) or alter potassium current (horizontal violet arrow). Morphological differentiation is accompanied by the up-regulation of whole-cell chloride conductance (up yellow arrow), enhanced RVD capabilities (up green arrow), and increased calcium signalling via IP_3 release from intracellular stores and through extracellular calcium entry via TRPV4 (up red arrows). We hypothesize that $[Ca^{2+}]_i$ released via IP_3 path can bind TRPV4 and sensitize it to cell volume variations to initiate RVD. B) Scheme of experimental protocol (1) and of patch-clamp experiments (2) performed at 3DIV upon acute photostimulation (λ_{ex}=450 nm) of [1mM] fAuNCs-BSA treated astrocytes. 3- The photostimulation elicits a decrease in whole cell potassium current (down violet arrow), possibly duo to a photothermal effect (up red arrow, ΔT°C). We cannot rule out that temperature increase may affect calcium signalling through the thermosensitive TRPV4 channel or the IP_3 pathway.

Experimental Condition	N. trials	N. samples	N. cells
NT CTRL	**9**	**23**	**75**
[1mM] fAuNCs-BSA CTRL	**9**	**46**	**230**
NT 0 EXT-Ca^{2+}	**3**	**6**	**26**
[1mM] fAuNCs-BSA 0 EXT-Ca^{2+}	**3**	**6**	**39**
NT 2APB	**3**	**6**	**17**
[1mM] fAuNCs-BSA 2 APB	**3**	**6**	**14**
NT RN-1734	**3**	**6**	**48**
[1mM] fAuNCs-BSA RN-1734	**3**	**6**	**43**

Table Supplementary 1. Statistics of calcium imaging experiments performed in fAuNCs-BSA –treated astrocytes. Number of experimental trials, replicates and cells analyzed for calcium imaging experiments performed on NT and fAuNCs-BSA [1mM] treated cells, for each condition.

Supporting references

1. Kim, H., Xue, X., Detection of Total Reactive Oxygen Species in Adherent Cells by 2',7'-Dichlorodihydrofluorescein Diacetate Staining. J Vis Exp. 2020, 160:10.3791/60682.
2. Eruslanov, E., Kusmartsev, S., Identification of ROS Using Oxidized DCFDA and Flow-Cytometry. Methods Mol Biol. 2010, 594, 57-72.